Determination of Optimal Locations and Parameters of Passive Harmonic Filters in Unbalanced Systems Using the Multiobjective Genetic Algorithm

Milos J. Milovanovic[1], Svetlana S. Raicevic[2], Dardan O. Klimenta[1,*], Nebojsa B. Raicevic[3], Bojan D. Perovic[1]

[1]Faculty of Technical Sciences, University of Pristina in Kosovska Mitrovica,
Kneza Milosa St. 7, RS-38220 Kosovska Mitrovica, Serbia
[2]IT, E-Communications and Development,
Post of Serbia, Vozda Karadjordja St. 13, RS-18101 Nis, Serbia
[3]Faculty of Electronic Engineering, University of Nis,
Aleksandra Medvedeva St. 14, RS-18000 Nis, Serbia
*milos.milovanovic@pr.ac.rs; svetlana.raicevic@posta.rs; *dardan.klimenta@pr.ac.rs;*
nebojsa.raicevic@elfak.ni.ac.rs; bojan.perovic@pr.ac.rs

Abstract—**This paper discusses the problem of optimal placement and sizing of passive harmonic filters to mitigate harmonics in unbalanced distribution systems. The problem is formulated as a nonlinear multiobjective optimisation problem and solved using the multiobjective genetic algorithm. The performance of the proposed algorithm is tested on unbalanced IEEE 13- and 37-bus three-phase systems. The optimal solutions are obtained based on the following objective functions: 1) minimisation of total harmonic distortion in voltage, 2) minimisation of costs of filters, 3) minimisation of voltage unbalances, and 4) a simultaneous minimisation of total harmonic distortion in voltage, costs of filters, and voltage unbalances. Finally, an analysis of the influence of uncertainties of load powers and changes in system frequency and filter parameters on filter efficiency was performed.**

Index Terms—**Genetic algorithm (GA); Optimisation; Passive harmonic filter (PHF); Unbalanced distribution system.**

I. INTRODUCTION

With the increase of nonlinear loads, harmonics injected into the distribution system and their effects become an issue of great importance. Most nonlinear loads of high powers often require harmonic reduction equipment to reduce harmonic currents, and therefore voltage distortions within the limits defined in the relevant standards. Depending on the desired solution, reduction of harmonics can be performed as an integral part of nonlinear equipment that contains inductors or as a separate part that includes passive and active filters. Each solution has its advantages and disadvantages, so it is not possible to define which one is the best. To avoid spending a large amount of money on an inappropriate and ineffective solution, it is necessary to first analyse the

problem and choose the most effective solution. Passive harmonic filters (PHFs) are the most frequently used due to their simplicity, high reliability and efficiency, small construction, and economical costs [1]. In addition to reducing harmonics, PHFs provide reactive power compensation, and therefore further improve the power quality. The major disadvantage of PHFs is that they are possible to have parallel resonances, and their performance depends on the impedance of the system. The exact value of the impedance at the point of common coupling is not known and is often not constant; it changes along with changes in the network configuration. Furthermore, PHFs are subject to readjustment (the so-called "detuning effect") due to changes in the system frequency and *R-L-C* parameters (due to ageing, temperature changes, and/or errors in the production process).

In the relevant scientific literature, there are only a few publications discussing the problem of optimal planning of PHFs in unbalanced distribution systems using metaheuristic methods. In [2], an optimal design of single-tuned PHFs of a modified IEEE 33-bus test system based on the genetic algorithm (GA) was discussed. The objective function included a reduction in the total harmonic distortion in voltage (THD_V). In [3], the GA and Monte Carlo simulation (MCS) method was proposed for optimal probabilistic planning of PHFs in unbalanced systems with high injection of photovoltaic (PV) generation to minimise filter costs, energy losses, and THD_V levels. In addition, in [4], the authors discussed a multiobjective optimal design of PHFs based on the non-dominated sorting genetic algorithm-II (NSGA-II). The objective functions included the minimisation of the THD_V levels, minimisation of voltage deviations, minimisation of PHF costs, minimisation of the frequency response index (FRI), and maximisation of the power factor in the system.

The calculation of the harmonic power flow (HPF), which is used for the evaluation of the objective function, is a key

segment in the planning of PHFs and harmonic analysis in general. In [5], the authors proposed a three-phase HPF method for unbalanced distribution systems that can be used for the optimal design of the PHF. This method performs better than the commonly used harmonic analysis methods based on the bus impedance or bus admittance matrices [6]–[8]. The accuracy of the HPF calculation depends on the applied method and then on the modelling of the system elements, the influence of the skin effect, and the phase angles of the current harmonics. Therefore, it is very important to provide this information in order to draw proper conclusions about the suitability of the chosen method.

In this paper, the multiobjective genetic algorithm (MOGA) for the optimal planning of single-tuned PHFs in unbalanced distribution systems is proposed. Different objective functions are considered taking into account minimisation of the THD_V, investment and operating costs of PHFs, and voltage unbalances. Harmonic levels are estimated using the decoupled harmonic power flow (DHPF) algorithm [7]. The proposed approach is tested on two unbalanced three-phase systems, i.e., the distorted IEEE 13- and 37-bus test systems.

The main contributions of this paper are as follows:
1. The procedure for the optimal planning of PHFs in unbalanced distribution systems using the MOGA-based approach is proposed;
2. The comparison of the HPF calculation results obtained in this paper with the available results from the literature and the results obtained using DIgSILENT software [9] is performed;
3. The effect of changing the system frequency and R-L-C parameters of the PHFs is analysed, as well as uncertainties of load powers, on the efficiency of the PHFs is made.

II. DESIGN OF PASSIVE FILTERS

Passive filters represent an appropriate combination of passive elements: inductors, capacitors, and resistors. The elimination or reduction of harmonics to the permitted limits is achieved by installing PHFs preferably close to the harmonic sources, where the appropriate selection of the R-L-C elements excites resonance in the circuit, and thus prevents the propagation of harmonics into the system. In practice many types of PHF can be found, including band-pass filters (single-tuned and double-tuned) and high-pass filters (first-order, second-order, third-order, and C-type).

The impedance of the single-tuned filters considered in this paper, at any angular frequency ω, can be expressed as follows

$$\underline{Z}_f^{(h)} = R + j\omega L + \frac{1}{j\omega C}, \tag{1}$$

where R is the resistance of the filter in Ω, C is the capacitance of the filter in F, L is the inductance of the filter in H, and h is the harmonic number.

The parameters important for the design of a single-tuned filter can be defined by the following equations [1]:

$$X_C = \frac{V_L^2}{Q_f}\left(\frac{h_r^2}{h_r^2 - 1}\right), \tag{2}$$

$$X_L = \frac{X_C}{h_r^2}, \tag{3}$$

$$C = \frac{1}{\omega_1 X_C}, \tag{4}$$

$$L = \frac{X_L}{\omega_1}, \tag{5}$$

$$R = \frac{h_r X_L}{Q}, \tag{6}$$

where Q_f is the nominal power of the filter in MVAr, V_L is the nominal (line-to-line) voltage of the filter in kV, h_r is the tuned harmonic order, X_L is the inductor reactance in Ω, X_C is the capacitor reactance in Ω, ω_1 is the fundamental angular frequency in rad/s, and Q is the quality factor of the filter. For single-tuned filters, a typical range for Q is between 50 and 150.

III. PROBLEM FORMULATION

The solution to the problem of optimal placement and sizing of PHFs aims to minimise/maximise the selected objective function $F(\mathbf{x}, \mathbf{u})$ through the optimal settings of the control variables $\mathbf{u}$, from the feasible space $\mathbf{U}$, while satisfying various the equality $g(\mathbf{x}, \mathbf{u}) = 0$ and inequality $h(\mathbf{x}, \mathbf{u}) \leq 0$ constraints. This mathematical principle can be expressed as follows:

$$\min/\max F(\mathbf{x},\mathbf{u}), \tag{7}$$

$$g(\mathbf{x},\mathbf{u}) = 0, \tag{8}$$

$$h(\mathbf{x},\mathbf{u}) \leq 0, \tag{9}$$

$$\mathbf{u} \in \mathbf{U}, \tag{10}$$

where $\mathbf{x}$ is a vector of dependent variables.

The vector of dependent variables $\mathbf{x}$ consists of the root mean square (RMS) bus voltages (V_{RMS}), total and individual harmonic distortions in voltage (THD_V and IHD_V), RMS currents flowing through the filter inductors (I_L^{RMS}) and capacitors (I_C^{RMS}), RMS and peak voltages across the filter capacitors (V_C^{RMS} and V_C^{peak}), and reactive powers of the filter capacitors (Q_C). Accordingly, the vector $\mathbf{x}$ can be defined as

$$\mathbf{x} = \lfloor V_{RMS,1}, ..., V_{RMS,N_b}, THD_{V,1}, ..., THD_{V,N_b},$$
$$IHD_{V,1}, ..., IHD_{V,N_b}, I_{L,1}^{RMS}, ..., I_{L,N_f}^{RMS}, I_{C,1}^{RMS}, ..., I_{C,N_f}^{RMS},$$
$$V_{C,1}^{RMS}, ..., V_{C,N_f}^{RMS}, V_{C,1}^{peak}, ..., V_{C,N_f}^{peak}, Q_{C,1}, ..., Q_{C,N_f} \rfloor^{\mathbf{T}}, \tag{11}$$

where N_b and N_f are the total number of buses and PHFs in the system, respectively.

The vector of control variables $\mathbf{u}$ consists of the locations where PHFs can be installed (L), reactive powers of PHFs (Q_f), types of PHFs (TF), tuned harmonic orders (h_r), and quality factors of PHFs (Q). Therefore, the vector $\mathbf{u}$ can be expressed as

$$\mathbf{u} = \lfloor L_1, ..., L_{N_f}, Q_{f,1}, ..., Q_{f,N_f}, TF_1, ..., TF_{N_f},$$
$$h_{r,1}, ..., h_{r,N_f}, Q_1, ..., Q_{N_f} \rfloor^{\mathbf{T}}. \tag{12}$$

A. Objective Functions

The problem of optimal placement and sizing of PHFs can be defined for different forms of objective functions. In this paper, the following objective functions are considered:

– *Minimisation of the maximum THD$_V$*

$$F_1 = \max\left(THD_V\right) = \max\left(\frac{1}{\left|\underline{V}_{i,p}^{(1)}\right|} \times \sqrt{\sum_{h=2}^{h_{\max}}\left|\underline{V}_{i,p}^{(h)}\right|^2} \times 100\right), \quad (13)$$

where $\underline{V}_{i,p}^{(h)}$ is the hth harmonic voltage in bus i ($i = 1, …, N_b$) for phase p($p = a, b, c$) and $h_{\max}$ is the maximum harmonic order considered.

– *Minimisation of the costs of PHFs*

$$F_2 = \sum_{i=1}^{N_f}\left(k_R R_i + k_L L_i + k_C C_i + k_Q Q_{F,i} + k_P P_{F,i}\right), \quad (14)$$

where R_i, L_i, C_i, $Q_{F,I}$, and $P_{F,i}$ are the resistance in Ω, inductance in mH, capacitance in µF, reactive power injection in kVAr, and power loss at the fundamental frequency in kW of the ith PHF, respectively, while k_R, k_L, k_C, k_Q, and k_P are the appropriate cost weighting coefficients. The values of these coefficients are as follows [10]: $k_R = 5$ p.u./Ω, $k_L = 3$ p.u./mH, $k_C = 2$ p.u./µF, $k_Q = 0.1$ p.u./kVAr, and $k_P = 0.1$ p.u./kW. Investment costs are determined by the values of R, L, and C elements, as well as the reactive power of the filter. Operating costs depend on active power losses during filter operation.

– *Minimisation of the maximum voltage unbalance factor*

$$F_3 = \max\left(VUF\right) = \max\left(\frac{\left|\underline{V}_{2,i}^{(1)}\right|}{\left|\underline{V}_{1,i}^{(1)}\right|} \times 100\right), \quad (15)$$

where VUF is the voltage unbalance factor, while $\underline{V}_{1,i}^{(1)}$ and $\underline{V}_{2,i}^{(1)}$ are the fundamental frequency positive-sequence and negative-sequence voltages at three-phase bus i calculated using the line-to-ground voltages $\underline{V}_{a,i}$, $\underline{V}_{b,I}$, and $\underline{V}_{c,i}$ as follows:

$$\underline{V}_{1,i}^{(1)} = \frac{1}{3}\left(\underline{V}_{a,i}^{(1)} + \underline{a}\underline{V}_{b,i}^{(1)} + \underline{a}^2\underline{V}_{c,i}^{(1)}\right), \quad (16)$$

$$\underline{V}_{2,i}^{(1)} = \frac{1}{3}\left(\underline{V}_{a,i}^{(1)} + \underline{a}^2\underline{V}_{b,i}^{(1)} + \underline{a}\underline{V}_{c,i}^{(1)}\right). \quad (17)$$

In (16) and (17), $\underline{a} = 1\angle 120°$ is the phasor rotation operator.

B. Constraints

The equality constraints (8) include the nonlinear balance equations of the power flow for the fundamental harmonic and constraints related to the harmonic power flow. In this paper, the backward-forward sweep (BFS) method [11] and the decoupled harmonic power flow (DHPF) method [7] were used to calculate unknown parameters of interest at the fundamental and harmonic frequencies, respectively.

Inequality constraints (9) represent the operating limits of dependent variables. These constraints take into account voltage quality limits in all system buses and limits of filter component design and operation.

Voltage quality limits include:
– limits on voltage magnitudes

$$V_{RMS}^{\min} \leq V_{RMS,i,p} \leq V_{RMS}^{\max}, \quad (18)$$

– limits on voltage harmonic distortions:

$$IHD_{V,i,p}^{(h)} \leq IHD_V^{\max,h}, \quad (19)$$

$$THD_{V,i,p} \leq THD_V^{\max}, \quad (20)$$

where $V_{RMS}^{\min} = 0.9$ p.u. and $V_{RMS}^{\max} = 1.1$ p.u. are the minimum and maximum bus voltage limits, respectively; $THD_V^{\max} = 5\%$ is the maximum acceptable level of the THD_V at any bus i and any phase p; $IHD_V^{\max,h} = 3\%$ is the maximum acceptable level of the IHD_V at the hth harmonic. The voltage quality limits are defined in the IEEE-519 standard [12].

The voltage and current limits in the components (capacitors and inductors) of the PHF in bus i at phase p, defined in the IEEE-1513 standard [13], are as follows:

$$V_{C,i,p}^{RMS} \leq 1.1\left(V_{C,i,p}^{rated}\right), \quad (21)$$

$$V_{C,i,p}^{peak} \leq 1.2\sqrt{2}\left(V_{C,i,p}^{rated}\right), \quad (22)$$

$$I_{C,i,p}^{RMS} \leq 1.35\left(I_{C,i,p}^{rated}\right), \quad (23)$$

$$Q_{C,i,p} \leq 1.35\left(Q_{C,i,p}^{rated}\right), \quad (24)$$

$$I_{L,i,p}^{RMS} \leq 1.35\left(I_{L,i,p}^{rated}\right), \quad (25)$$

where $V_{C,i,p}^{rated}$, $I_{C,i,p}^{rated}$, and $Q_{C,i,p}^{rated}$ are the rated values of the voltage, current, and power of the PHF capacitor in bus i at phase p, respectively, and $I_{L,i,p}^{rated}$ is the rated value of the current flowing through the PHF inductor in bus i at phase p.

Constraints (10) define the feasible region of control variables, i.e., locations where PHFs can be installed, as well as powers, types, tuned harmonic orders, and quality factors of PHFs. All buses and phases in an unbalanced distribution system represent potential locations for the placement of PHFs. The reactive power supplied by PHFs should not exceed the system demand. Therefore, the upper limit of the total power supplied by the PHFs is introduced to avoid the problem of overcompensation. In this paper, several PHFs are considered. The control variable *TF* can have a value of 1, 2, or 3, which corresponds to the single-tuned PHF for the third-order harmonic, single-tuned PHF for the fifth-order harmonic, and single-tuned PHF for the seventh-order harmonic, respectively. An analysis of the impact of variations in the system frequency and variations in the reactance of inductors and capacitors (due to ageing, temperature changes, and/or error tolerances in the manufacturing process) on the performance of PHFs shows the importance of including the detuning effect in the design. Taking into account the above variations, the considered PHFs are tuned to a resonant frequency of 0.85h to 0.97h, which is in accordance with the IEEE-1531 standard [13]. The lower and upper limit values of the quality factor are 10 and 150, respectively [14]. The inequality constraints (9) are taken into account through quadratic penalty factors by

means of which the objective function F is expanded [1].

IV. OPTIMISATION ALGORITHM

A. *Multiobjective Optimisation Approach*

Multicriteria or multiobjective optimisation implies the optimisation of more than one objective function that is mutually contradictory, which means that the improvement of one cannot be achieved without worsening another. Therefore, the goal is to obtain a whole series of optimal solutions that imply mutual non-dominance. Such solutions are called Pareto-optimal solutions. Pareto-optimal solutions cannot be improved by one criterion without being worsened by another. In this sense, they represent a kind of global optimal solution. The set of all Pareto solutions to a problem is called a Pareto front. Based on the Pareto front, the designer gains a clear insight into the behaviour of the objective functions when changing individual parameters, so that he/she can choose the solution that represents the most acceptable compromise under the given conditions. The selection of the best solution from the set of Pareto-optimal solutions is made by one of the decision theories. During the last few years, many optimisation methods inspired by different natural processes have appeared, known as evolutionary algorithms, among which the most famous is MOGA. In general, a multiobjective optimisation problem can be defined as

$$\min F(\mathbf{x}, \mathbf{u}) = \left[F_1(\mathbf{x}, \mathbf{u}), F_2(\mathbf{x}, \mathbf{u}), ..., F_m(\mathbf{x}, \mathbf{u}) \right]^T \quad (26)$$

under constraints (8)–(10).

It can be said that $\mathbf{u}^*$ is a Pareto solution if there is no other decision vector $\mathbf{u} \in \mathbf{U}$ such that $f_j(\mathbf{u}) \le f_j(\mathbf{u}^*)$ for all functions $j = 1, 2, ..., m$ and $f_j(\mathbf{u}) < f_j(\mathbf{u}^*)$ for at least one function f_j. When solving multicriteria problems, two conceptually different problems can be identified:

1. Searching the space of feasible solutions;
2. Decision making.

The first aspect refers to the optimisation process in which a set of solutions that meet the criteria for a Pareto-optimal solution is obtained. The second aspect refers to the problem of choosing a suitable compromise solution from a set of solutions that satisfy the Pareto-optimal criterion.

The main disadvantage of GA [1]–[3] is that it cannot be directly applied to multicriteria problems, because it allows the optimisation of only one objective function, so it must be executed as many times as the optimal solutions are desired. To obtain Pareto-optimal solutions in that case, the principle of weighting factors can be used. A much better way to solve these problems is to use the MOGA-based approach. The application of this approach to solving the problem of determining optimal locations and parameters of PHFs can be defined in the following steps:

1. Representing a group of chromosomes (i.e., individuals);
2. Initialisation of each chromosome in the population;
3. Calculating the fitness of each chromosome;
4. Selection;
5. Crossing;
6. Mutation;
7. Checking the stopping criteria.

Fitness calculation is based on harmonic analysis performed using the DHPF algorithm [7]. The procedure of searching for an optimal solution consists of an iterative repetition of steps from 3 to 7 until the stopping criterion is reached. The stopping criterion may include the maximum number of iterations (generations) or a termination tolerance on the fitness value. More details on GA can be found in [1]–[4].

B. *Programme Realization of the MOGA-Based Approach*

The chromosome structure when determining the optimal locations and parameters of the PHFs using a MOGA-based approach is presented in Table I. The positions are given in the second row of the table and names of the variables used in the third.

TABLE I. CHROMOSOME STRUCTURE FOR OPTIMAL PHF DESIGN

Locations	Sizes	Types	Tuned orders	Quality factor
$1, ..., N_f$	$N_f + 1, ..., 2N_f$	$2N_f + 1, ..., 3N_f$	$3N_f + 1, ..., 4N_f$	$4N_f + 1, .., 5N_f$
$L_1,...,L_{N_f}$	$Q_{f,1},...,Q_{f,N_f}$	$TF_1,...,TF_{N_f}$	$h_{r,1},...,h_{r,N_f}$	$Q_1,...,Q_{N_f}$

The algorithm was run on a PC with an AMD Ryzen 7 3700U processor with 12 GB RAM. To execute the MOGA, a programme implementation was used in the MATLAB software within the optimisation toolbox (*optimtool*) module. To compare the results, four different analyses were conducted. First, individual objective functions (Case 1 - F_1, Case 2 - F_2, and Case 3 - F_3) were considered separately using single-objective optimisation. In the last, fourth, case, simultaneous optimisation of all three functions was considered. Values of the objective functions analysed have different units and different orders of magnitude, making comparison difficult. Thus, it is necessary to normalise them so that they all have similar orders of magnitude. The normalisation of an objective function can be done in the following manner

$$f_{i,j}^{norm} = \frac{F_{i,j} - F_i^{\min}}{F_i^{\max} - F_i^{\min}}, \quad (27)$$

where $f_{i,j}^{norm}$ and $F_{i,j}$ represent the normalised value and the actual value of the ith objective function ($i = 1, 2, 3$) of the jth solution from the Pareto-optimal front, while $F_i^{\min}$ and $F_i^{\max}$ are the minimum and maximum values of the ith objective function, respectively. The MOGA parameters used are presented in Table II.

TABLE II. PARAMETERS OF THE MOGA-BASED APPROACH.

Parameters	Values and/or functions
Number of generations	100
Population size	250
Selection function, size	Tournament, 2
Crossover fraction	0.8
Crossover function, ratio	Intermediate, 1
Mutation function	Adaptive feasible
Distance measure function	Distancecrowding
Pareto front population fraction	0.35

V. RESULTS AND DISCUSSION

The proposed method was evaluated using IEEE 13- and 37-bus unbalanced three-phase systems. At the fundamental frequency, all loads are represented using the constant power model, the constant impedance model, or the constant current model. At harmonic frequencies, linear loads are modelled by the series RL impedance model, and nonlinear loads are treated as harmonic current sources. PHFs are modelled as constant impedances connected in a grounded wye. For each objective function under consideration, a sequence of 10 consecutive runs was performed, and the results presented here represent the best values obtained.

A. Simulations on the IEEE 13-Bus Test System

The three-phase configuration of the IEEE 13-bus test system is shown in Fig. 1, while complete data can be found in [15]. This system is used as a benchmark for the development of novel harmonic analysis algorithms and for the evaluation of existing harmonic software. The system is a small radial and highly unbalanced system operating at 4.16 kV. The total active and reactive powers are 3.466 MW and 2.102 MVAr, respectively. The original IEEE 13-bus system contains voltage transformers, regulators, single-phase and three-phase lines and cables, capacitors, spot, and distributed loads. The harmonic sources in this system are fluorescent light banks, adjustable speed drivers (ASDs), and composite loads. The harmonic spectra of nonlinear loads are available in [16]. It is assumed that the substation voltage in all three phases has the same magnitude of 1 p.u. and that the substation voltage does not contain harmonics.

The HPF results are verified by comparing them with the available results of the works in [6], [8], [17] and the results obtained using DIgSILENT software [9]. Taking into account the fact that the results of HPF calculations may differ due to the application of different models of linear loads, Table III

shows THD_V solutions obtained using the series and parallel models.

The reason for making comparisons is to demonstrate the accuracy of the DHPF method, which was used to evaluate the objective functions. The phase angles of the current harmonics are neglected. Without the phase information of the harmonic current sources, the results can be considered the worst case for harmonic analysis [5]. In this way, one gets to the safety side of the calculation.
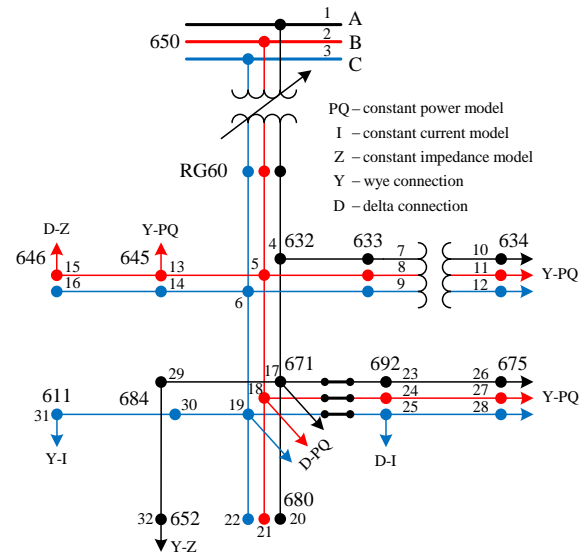

Fig. 1. Three-phase diagram of the IEEE 13-bus test system.

The accuracy of the HPF calculation depends on the applied method and then on the modelling of the system elements, the influence of the skin effect, and the phase angles of the current harmonics. Table III shows a very high degree of consistency between the results obtained by the DHPF method and the DIgSILENT software.

TABLE III. COMPARISON OF THE THD_V LEVELS.

Bus	Phase and node	HPF [6]	HPF [8]	HPF [17]	DIgSILENT 15.1.6 software	DHPF with series model	DHPF with parallel model
650	A, 1	0	0	0	0	0	0
	B, 2	0	0	0	0	0	0
	C, 3	0	0	0	0	0	0
632	A, 4	1.890	2.031	1.917	2.400	2.291	2.403
	B, 5	1.000	1.841	0.497	1.500	1.635	1.723
	C, 6	2.280	2.221	2.274	2.500	2.412	2.486
633	A, 7	1.880	2.015	1.910	2.400	2.276	2.391
	B, 8	0.990	1.827	0.492	1.500	1.622	1.714
	C, 9	2.270	2.206	2.265	2.500	2.398	2.473
634	A, 10	1.860	1.980	1.880	2.300	2.243	2.380
	B, 11	0.980	1.807	0.487	1.500	1.607	1.711
	C, 12	2.260	2.180	2.241	2.500	2.374	2.468
645	B, 13	1.060	1.990	0.499	1.500	1.670	1.774
	C, 14	2.320	2.271	2.277	2.500	2.459	2.514
646	B, 15	1.100	2.076	0.500	1.600	1.689	1.801
	C, 16	2.360	2.305	2.282	2.500	2.492	2.536
671	A, 17	4.020	4.142	4.062	5.100	4.874	5.078
	B, 18	1.960	3.389	1.036	3.100	3.244	3.356
	C, 19	4.910	4.696	4.941	5.400	5.258	5.437
680	A, 20	4.020	4.142	4.062	5.100	4.874	5.078
	B, 21	1.960	3.389	1.036	3.100	3.244	3.356
	C, 22	4.910	4.696	4.941	5.500	5.258	5.436
692	A, 23	4.020	4.142	4.062	5.100	4.874	5.078
	B, 24	1.960	3.389	1.036	3.100	3.244	3.356
	C, 25	4.910	4.696	4.941	5.500	5.258	5.436
675	A, 26	4.280	4.267	4.313	5.400	5.134	5.361
	B, 27	1.970	3.416	1.049	3.100	3.293	3.408
	C, 28	5.050	4.794	5.069	5.700	5.437	5.614
684	A, 29	4.070	4.186	4.077	5.200	4.944	5.151
	C, 30	5.070	4.776	5.074	5.600	5.388	5.580
611	C, 31	5.230	4.850	5.226	5.700	5.509	5.716
652	A, 32	4.130	4.232	4.090	5.200	5.016	5.218

The mean absolute relative errors between the THD_V values obtained using the DHPF method and the DIgSILENT software are less than 5 % (i.e., 4.31 % for the series model and 3.94 % for the parallel model). Furthermore, the table indicates that the results generated by the DHPF method agree well with those reported in [6], [8], and [17]. This observation is illustrated by the diagram in Fig. 2.
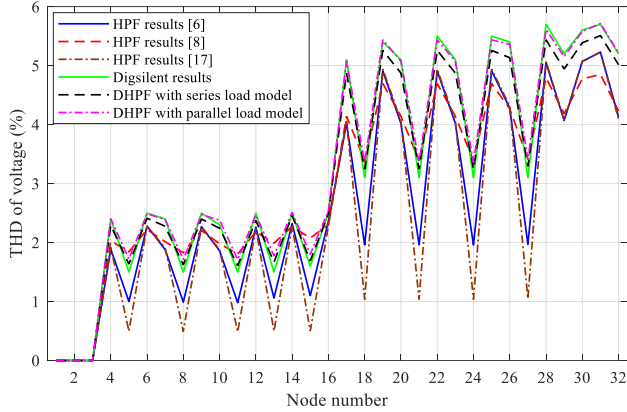

Fig. 2. Comparisons between the THD_V levels of the IEEE 13-bus system.

The problem of designing PHF parameters was considered with three filters, and the results obtained were then compared with those generated in the case when there are no filters in the system. For each PHF, the size is set between 0 MVAr and 1 MVAr. It is also assumed that the upper limit of the total power supplied by the PHFs equals 2.1 MVAr. The optimal settings of the PHF parameters are listed in Table IV, while the values of the dependent variables and the objective functions are presented in Table V. The best values of the objective function for the considered cases are highlighted in bold.

TABLE IV. LOCATIONS AND PARAMETERS OF INSTALLED FILTERS FOR THE IEEE 13-BUS TEST SYSTEM.

Optimal filter design parameters						
Bus and phase	Q_f (MVAr)	h_r	Q	R (Ω)	L (mH)	C (μF)
Case 1						
675a	0.927	2.910	145.519	0.017	2.211	375.938
675b	0.279	2.877	135.668	0.060	7.529	112.879
675c	0.866	2.903	62.484	0.042	2.379	350.958
Case 2						
675b	0.055	2.905	149.510	0.275	37.475	22.247
675c	0.252	2.882	149.072	0.061	8.313	101.918
Case 3						
680a	0.938	2.822	133.035	0.019	2.343	377.116
680c	0.478	2.598	70.627	0.077	5.569	187.243
611c	0.168	2.730	115.438	0.126	14.124	66.866
Case 4						
692a	0.769	2.852	67.157	0.045	2.789	310.055
692c	0.571	2.901	89.662	0.044	3.611	231.462

TABLE V. VALUES OF DEPENDENT VARIABLES AND OBJECTIVE FUNCTIONS FOR THE IEEE 13-BUS SYSTEM.

Dependent variables and objective functions	Base case	Case 1	Case 2	Case 3	Case 4
Min. V_{RMS} (p.u.)	0.867	0.929	0.900	0.900	0.900
Max. V_{RMS} (p.u.)	1.000	1.022	1.000	1.078	1.013
Max. IHD_V (%)	5.331	0.584	2.980	1.669	0.709
$\sum P_F$ (kW)	-	8.088	0.682	6.319	6.723
$\sum Q_F$ (MVAr)	-	1.995	0.258	1.619	1.259
P_{loss} (kW)	148.18	123.31	132.65	145.86	124.13

Dependent variables and objective functions	Base case	Case 1	Case 2	Case 3	Case 4
F_1 (%)	5.514	**0.774**	3.641	1.872	**1.205**
F_2 (p.u.)	-	1916.78	**413.26**	1492.25	**1229.24**
F_3 (%)	2.745	1.462	2.935	**0.423**	0.775

As can be seen from Table V, in relation to the base case, the maximum THD_V level in Case 1 can be reduced from 5.514 % to 0.774 % if three PHFs are installed on bus 675. This solution requires the highest costs. Filters are tuned to eliminate the most dominant harmonic, i.e., the third-order harmonic (Fig. 3). In Case 2, the optimal PHF design has the lowest costs. The maximum VUF in the distribution system without PHF amounts to 2.745 % and can be reduced to a minimum of 0.423 % if three single-tuned PHFs are used, as in Case 3. Furthermore, observing the power losses from Table V, it is clear that the optimal design of PHFs, in addition to suppression of harmonics, can lead to a significant reduction in losses in the whole system.

In Case 4, the objective function maintains a balance between the three objectives. The selection of the appropriate Pareto-optimal solution was made based on the criteria

$$\min \sum_{i=1}^{3} f_i^{norm}. \qquad (28)$$

Compared to the base case, the best compromise solution shows a reduction of 78.15 % in the maximum THD_V level and a reduction of 71.77 % in the maximum VUF. The graphical representation of the points of the Pareto-optimal front for Case 4 is given in Fig. 4 and provides the designer with sufficient information about the mutual connection of objective functions, as well as the distance of the optimal solutions in the space of the objective functions.
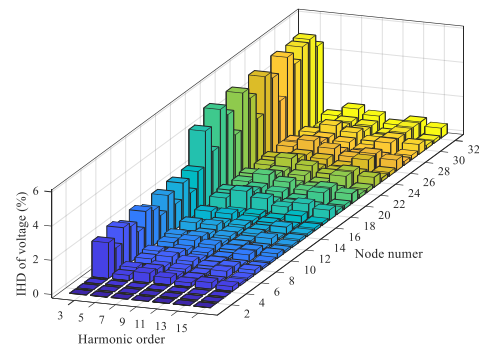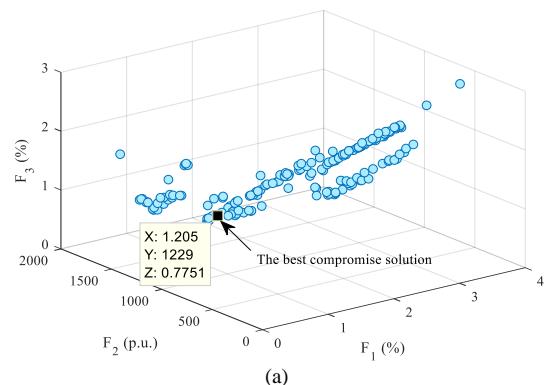

Fig. 3. Voltage harmonics at each node of the IEEE 13-bus test system for the base case.
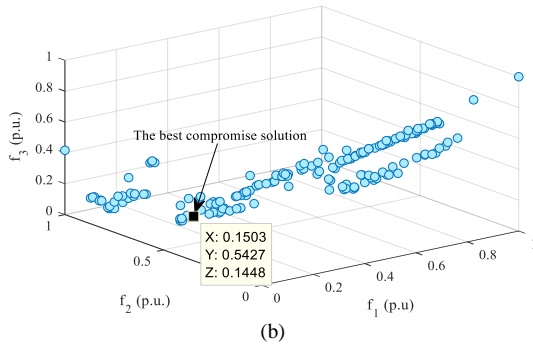

(a)

(b)

Fig. 4. Pareto front for Case 4: (a) actual values and (b) normalised values of the objective functions.

From Table V, it can also be observed that the voltage magnitudes and IHD_V values meet the limits defined in the IEEE-519 standard. Comparisons between the THD_V levels and between the corresponding voltage profiles at nodes of the IEEE 13-bus test system are shown in Figs. 5 and 6, respectively. The average running time of the MOGA-based approach was about 30 min.
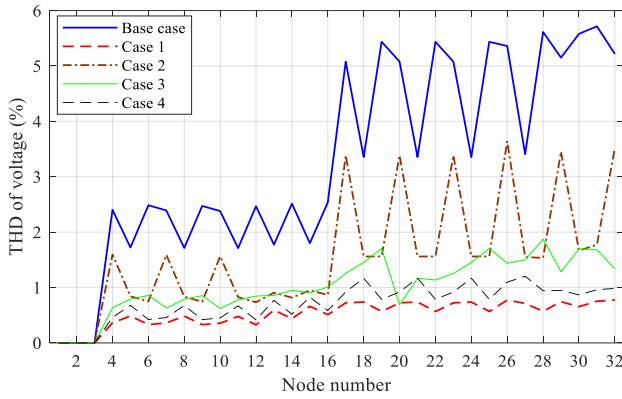

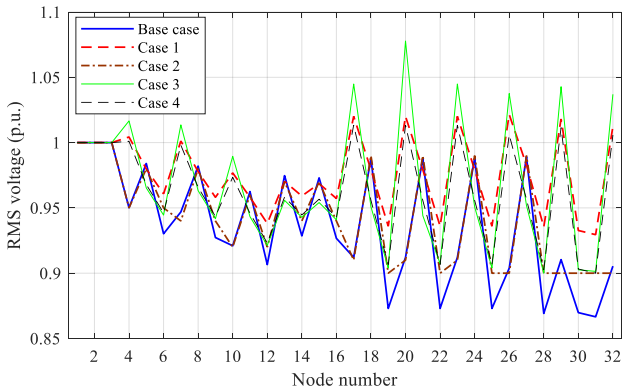Fig. 5. THD_V levels of the IEEE 13-bus system with and without PHFs.

Fig. 6. Voltage profiles of the IEEE 13-bus system with and without PHF.

B. Simulations on the IEEE 37-Bus Test System

The second system studied is the IEEE 37-bus system shown in Fig. 7.

It is a three-phase system operating at 4.8 kV with unbalanced loads of the single and three phases. To investigate the impact of harmonics, it is assumed that a wye-connected nonlinear load (i.e., ASD type) is connected at bus 740. The complex phase powers of this load are as follows: Sa = (250 + j187.5) kVA, Sb = (150 + j112.5) kVA, and Sc = (350 + j262.5) kVA. It is assumed that all phase voltages of the substation are equal and amount to 1 p.u. The specified type, location, and power of nonlinear load are arbitrarily

chosen. However, it is possible to carry out simulations for any other type of nonlinear loads (i.e., any harmonic spectrum) and any combination of locations and powers of nonlinear loads. The total active and reactive powers in the system are 3.205 MW and 1.764 MVAr, respectively. For each PHF, the size is set between 0 MVAr and 1 MVAr, and the upper limit of the total power supplied by the PHFs is equal to the total reactive power of all loads.
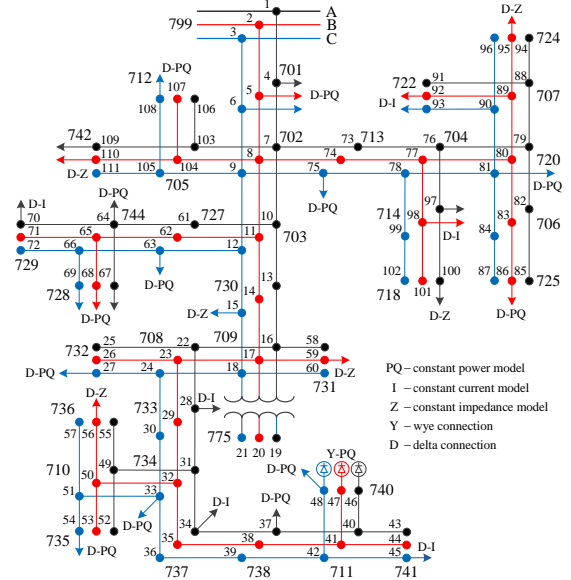

Fig. 7. Three-phase diagram of the IEEE 37-bus test system.

The optimal settings of the PHF parameters are presented in Table VI, while the values of the dependent variables and objective functions are listed in Table VII.

TABLE VI. LOCATIONS AND PARAMETERS OF INSTALLED FILTERS FOR THE IEEE 37-BUS TEST SYSTEM.

Optimal filter design parameters						
Bus and phase	Q_f (MVAr)	h_r	Q	R (Ω)	L (mH)	C (µF)
Case 1						
740a	0.441	2.884	63.514	0.108	6.308	134.097
740b	0.276	2.880	11.439	0.962	10.134	83.686
740c	0.981	2.908	149.760	0.020	2.785	298.759
Case 2						
740a	0.283	2.901	128.195	0.083	9.694	86.225
740b	0.139	2.801	105.742	0.214	21.408	41.890
740c	0.275	2.894	134.525	0.082	10.049	83.583
Case 3						
740a	0.906	2.836	80.933	0.042	3.192	274.131
740b	0.467	2.792	87.679	0.077	6.422	140.509
740c	0.381	2.852	98.622	0.082	7.505	115.300
Case 4						
740a	0.289	2.872	81.569	0.129	9.738	87.584
740b	0.202	2.778	90.823	0.173	15.024	60.692
740c	0.353	2.904	81.079	0.105	7.767	107.453

As can be seen from Table VII, in the base case, the maximum THD_V level, total power losses, and maximum VUF value in the system are 12.253 %, 211.26 kW, and 2.362 %, respectively. Additionally, the minimum RMS bus voltage and the maximum THD_V level violate the allowable limits defined in the IEEE-519 standard. In Case 1, the maximum THD_V level is reduced by 77.76 %, but the maximum VUF value is increased by 71.55 %. This solution requires the highest costs of PHFs of 1251.95 p.u. The

minimum costs of the PHFs are achieved in Case 2, and the minimum *VUF* value is obtained in Case 3. Case 4 can be taken as the optimal compromise solution obtained using (28). The Pareto-optimal front is given in Fig. 8. For this system, for all cases, the MOGA-based approach always gives the same locations to install PHFs. This is because the distortion is the largest on bus 740.

TABLE VII. VALUES OF DEPENDENT VARIABLES AND OBJECTIVE FUNCTIONS FOR THE IEEE 37-BUS SYSTEM.

| Dependent variables and objective functions	Base case	Case 1	Case 2	Case 3	Case 4
Min. V_{RMS} (p.u.)	0.896	0.944	0.907	0.902	0.915
Max. V_{RMS} (p.u.)	1.000	1.000	1.000	1.014	1.000
Max. IHD_V (%)	10.969	1.584	2.679	2.624	2.460
$\sum P_F$ (kW)	-	13.350	1.882	7.597	3.457
$\sum Q_F$ (MVAr)	-	1.544	0.593	1.601	0.726
P_{loss} (kW)	211.26	190.55	147.28	191.81	142.72
F_1 (%)	12.253	**2.725**	4.980	4.806	**4.439**
F_2 (p.u.)	-	1251.95	**608.23**	1273.09	**684.03**
F_3 (%)	2.362	4.052	2.033	**0.487**	**2.276**

(a)

(b)
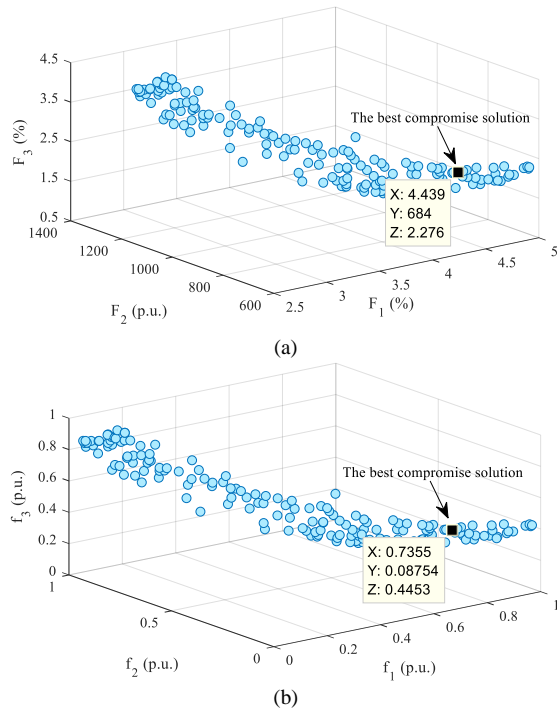
Fig. 8. Pareto front for Case 4: (a) actual values and (b) normalised values of the objective functions.

Figures 9 and 10 show the THD_V levels and voltage profiles at the nodes of the system before and after PHF placement.
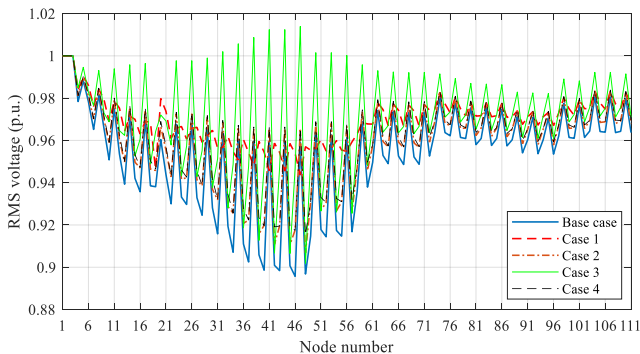

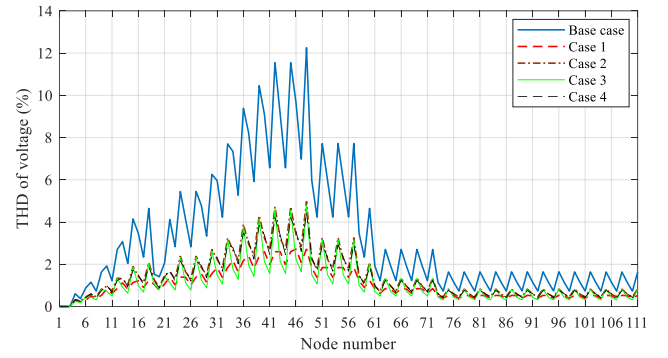Fig. 9. THD_V levels of the IEEE 37-bus system with and without PHF.

Fig. 10. Voltage profiles of the IEEE 37-bus system with and without PHFs.

According to these results, it can be seen that after PHF placement, RMS values of voltages and THD_V levels at all nodes are within the allowed limits. As the MOGA algorithm is a stochastic search algorithm, it cannot be guaranteed that the obtained solutions are global optimum, but they can certainly be considered as local optimum. The average running time of the MOGA in the case of the IEEE 37-bus system was about 90 min.

C. The Effect of Changing the Input Parameters on the Result of HPF Calculations

The efficiency of a filter is largely dependent on the impedance of the system at the point of its connection, as well as changes in the frequency of the system and the parameters of the filter *R-L-C*. In this section, the Monte Carlo Simulation (MCS) method [18] is used to obtain statistical information for the output variables of interest, such as voltage distortions. Uncertainties of the load powers (*P* and *Q*) are taken into consideration, and the normal or Gaussian distribution is used to represent the active and reactive powers of the loads. The mean values of the load powers are adopted as equal to the rated powers given in [15], and subject to the normal distribution with a standard deviation of 10 %. Furthermore, the *R-L-C* parameters of the PHFs are subject to the variations from their rated values due to ageing, manufacturing tolerances, and ambient temperature variations. The capacitance variation is dominated by the manufacturing tolerance. For single-tuned PHFs, the IEEE-1531 standard recommends the selection of capacitors with tolerance in the range ±5 % and inductors with tolerance in the range ±3 %. Although the IEEE-1531 standard does not state a tolerance for the resistance, some authors use ±3 % to model it [19]. Variation in system frequency is represented by a normal distribution with a tolerance in the range ±1 %.

For all case studies, the MCS method performs 5,000 HPF calculations. This number of samples is high enough to guarantee the convergence of the MCS. Table VIII shows the maximum, mean, and standard deviation (STD) values for a selected set of output variables of interest (i.e., the THD_V levels on bus 740). In addition, to show the impact of individual input random variables on the statistical characteristics of HPF results, probabilistic HPF calculations were performed for different combinations of input random variables, as presented in Table VIII.

The corresponding THD_V levels at all nodes of the IEEE 37-bus system are shown in Figs. 11 and 12. The deterministic HPF is marked with a red line, and the probabilistic HPFs are marked with other lines. From these

results, it can be seen that the *R-L-C* parameters of the PHF, as input variables, have a higher impact on the standard deviation of the output variables than variables *P*, *Q*, and *f*. In addition, it is evident that in some cases there may be an increase in the *THD_V* values, which occurs as a result of the resonance between the filter capacitors and the inductive reactance of the system.
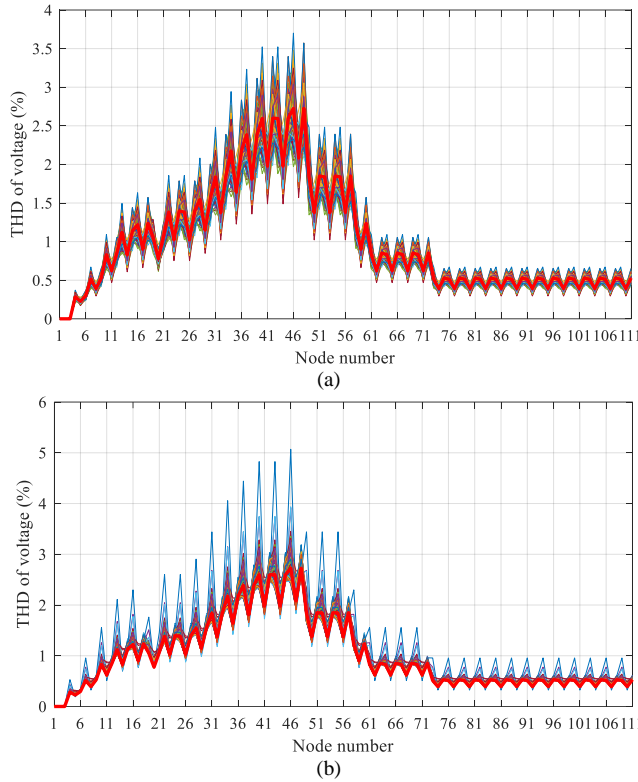

Fig. 11. Comparisons between *THD_V* levels for Case 1: (a) *P* and *Q* are input variables and (b) the *R-L-C* parameters of the PHF are input variables.
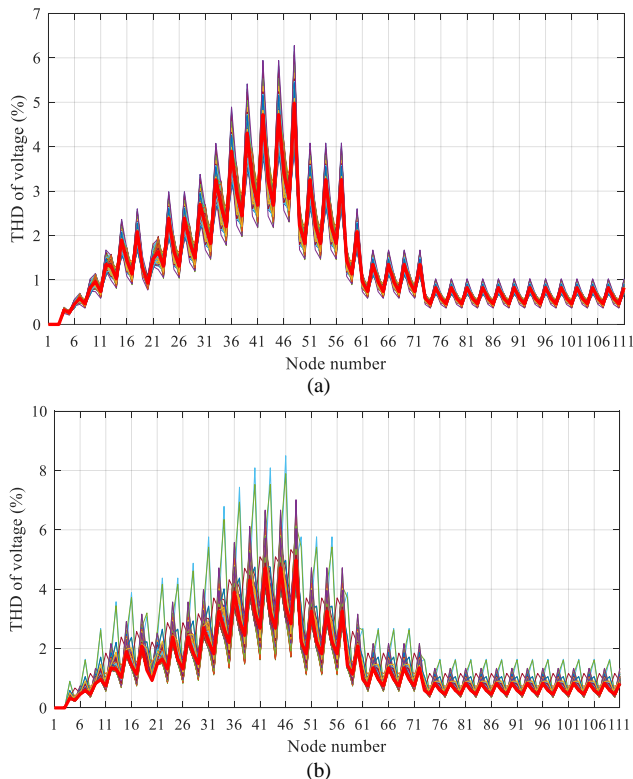

Fig. 12. Comparisons between *THD_V* levels for Case 2: (a) *P* and *Q* are input variables and (b) the *R-L-C* parameters of the PHF are input variables.

TABLE VIII. MAXIMUM, MEAN, AND STANDARD DEVIATION VALUES OF THD_V LEVELS AT BUS 740.

THD_V on bus 740 (%)		Input random variables				
		P, Q	*f*	*R, L, C*	*f, R, L, C*	*P, Q, f, R, L, C*
Case 1						
Phase *a*, Node 46	Max	3.702	3.069	5.069	3.966	5.102
	Mean	2.725	2.726	2.761	2.770	2.769
	STD	0.229	0.097	0.237	0.252	0.341
Phase *b*, Node 47	Max	2.557	2.272	3.384	3.241	4.172
	Mean	2.100	2.085	2.122	2.121	2.140
	STD	0.112	0.055	0.141	0.145	0.220
Phase *c*, Node 48	Max	3.398	2.944	3.747	3.473	3.857
	Mean	2.747	2.731	2.763	2.766	2.782
	STD	0.141	0.056	0.153	0.141	0.278
Case 2						
Phase *a*, Node 46	Max	4.795	4.795	8.497	10.984	12.568
	Mean	3.276	3.280	3.349	3.365	3.351
	STD	0.384	0.296	0.543	0.562	0.613
Phase *b*, Node 47	Max	3.603	3.176	5.332	6.615	7.108
	Mean	2.684	2.696	2.596	2.600	2.604
	STD	0.336	0.296	0.419	0.436	0.475
Phase *c*, Node 48	Max	6.651	6.218	7.015	13.912	13.991
	Mean	4.538	4.541	4.621	4.687	4.655
	STD	0.975	0.888	1.037	1.153	1.215

VI. CONCLUSIONS

The main conclusions arising from the results and discussion are as follows:

− It is shown that proper planning of PHFs, in addition to reducing harmonic distortions, can improve other technical and economic performances of unbalanced systems.

− The accuracy of the DHPF method is successfully verified using DIgSILENT software. The mean absolute relative errors between the THD_V values obtained using the DHPF method and those obtained using DIgSILENT are lower than 5 %, which means that the accuracy of this method is high.

− The R-L-C parameters of the PHFs, as input random variables, are found to have a greater impact on the standard deviation of the THD_V levels than load powers and frequency.

− The average running time of the MOGA-based approach in the cases of the IEEE 13- and 37-bus test systems was about 30 and 90 minutes, respectively.

− The proposed MOGA-based approach can be applied to any other unbalanced distribution system with any type of nonlinear loads and renewable energy sources.

Future directions of the research will be:

1. Development and/or application of other metaheuristic methods;

2. Taking into account the change of other input variables, such as magnitude and phase angle of harmonic sources, impedances of branches, etc.

3. Consideration of other types of filters, nonlinear loads and sources.

CONFLICTS OF INTEREST

The authors declare that they have no conflicts of interest.

REFERENCES

[1] M. Milovanović, J. Radosavljević, D. Klimenta, and B. Perović, "GA-based approach for optimal placement and sizing of passive power filters to reduce harmonics in distorted radial distribution systems", *Electrical Engineering*, vol. 101, pp. 787–803, 2019. DOI:

10.1007/s00202-019-00805-w.

[2] I. D. Melo, J. L. R. Pereira, A. M. Variz, and P. F. Ribeiro, "Allocation and sizing of single tuned passive filters in three-phase distribution systems for power quality improvement", *Electric Power Systems Research*, vol. 180, art. 106128, 2020. DOI: 10.1016/j.epsr.2019.106128.

[3] M. R. Jannesar, A. Sedighi, M. Savaghebi, A. Anvari-Moghaddam, and J. M. Guerrero, "Optimal probabilistic planning of passive harmonic filters in distribution networks with high penetration of photovoltaic generation", *International Journal of Electrical Power & Energy Systems*, vol. 110, pp. 332–348, 2019. DOI: 10.1016/j.ijepes.2019.03.025.

[4] J. Khajouei, S. Esmaeili, and S. M. Nosratabadi, "Optimal design of passive filters considering the effect of Steinmetz circuit resonance under unbalanced and non-sinusoidal conditions", *IET Generation, Transmission & Distribution*, vol. 14, no. 12, pp. 2333–2344, 2020. DOI: 10.1049/iet-gtd.2019.1755.

[5] J.-H. Teng, S.-H. Liao, and R.-C. Leou, "Three-phase harmonic analysis method for unbalanced distribution systems", *Energies*, vol. 7, no. 1, pp. 365–384, 2014. DOI: 10.3390/en7010365.

[6] N.-C. Yang and M.-D. Le, "Three-phase harmonic power flow by direct Z_{BUS} method for unbalanced radial distribution systems with passive power filters", *IET Generation, Transmission & Distribution*, vol. 10, no. 13, pp. 3211–3219, 2016. DOI: 10.1049/iet-gtd.2015.1368.

[7] M. Milovanović, J. Radosavljević, N. Arsić, and B. Perović, "A power flow method for unbalanced three-phase distribution networks with nonlinear loads", in *Proc. of 2022 21st International Symposium INFOTEH-JAHORINA*, 2022, pp. 1–6. DOI: 10.1109/INFOTEH53737.2022.9751281.

[8] B. Arabsalmanabadi, A. Javadi, and K. Al-Haddad, "Harmonic power flow in unbalanced and polluted radial distribution systems", in *Proc. of 2017 IEEE International Conference on Industrial Technology (ICIT)*, 2017, pp. 1504–1509. DOI: 10.1109/ICIT.2017.7915589.

[9] *DIgSILENT Version 15 User Manual*, Gomaringen, Germany, 2013.

[10] C.-J. Chou, C.-W. Liu, J.-Y. Lee, and K.-D. Lee, "Optimal planning of large passive-harmonic-filters set at high voltage level", *IEEE Transactions on Power Systems*, vol. 15, no. 1, pp. 433–441, 2000. DOI: 10.1109/59.852156.

[11] M. Milovanović, J. Radosavljević, and B. Perović, "A backward/forward sweep power flow method for harmonic polluted radial distribution systems with distributed generation units", *International Transactions on Electrical Energy Systems*, vol. 30, no. 5, p. e12310, 2020. DOI: 10.1002/2050-7038.12310.

[12] *IEEE Recommended Practices and Requirements for Harmonic Control in Electrical Power Systems*, IEEE Standard 519-1992, 1993.

[13] *IEEE Guide for Application and Specification of Harmonic Filters*, IEEE Standard 1531-2003, 2003.

[14] E. F. Fuchs and M. A. S. Masoum, *Power Quality in Power Systems, Electrical Machines, and Power-Electronic Drives*, 3rd ed., Academic Press, 2023, pp. 925–930. DOI: 10.1016/C2018-0-02457-3.

[15] IEEE PES distribution system analysis subcommittee's, Distribution test feeder working group, Test feeders resources. [Online]. Available: https://cmte.ieee.org/pes-testfeeders/resources/

[16] R. Abu-Hashim *et al.*, "Test systems for harmonics modeling and simulation", *IEEE Transactions on Power Delivery*, vol. 14, no. 2, pp. 579–587, 1999. DOI: 10.1109/61.754106.

[17] R. Satish, K. Vaisakh, A. Y. Abdelaziz, and A. El-Shahat, "A novel three-phase harmonic power flow algorithm for unbalanced radial distribution networks with the presence of D-STATCOM devices", *Electronics*, vol. 10, no. 21, p. 2663, 2021. DOI: 10.3390/electronics10212663.

[18] M. Milovanović, J. Radosavljević, B. Perović, and J. Vukašinović, "Probabilistic power flow calculation in asymmetric, unbalanced and distorted distribution networks", in *Proc. of 2023 10th International Conference on Electrical, Electronic and Computing Engineering (IcETRAN)*, 2023, pp. 1–6. DOI: 10.1109/IcETRAN59631.2023.10192117.

[19] I. Pérez Abril, "Passive filters' placement considering parameters' variations", *International Transactions on Electrical Energy Systems*, vol. 29, no. 2, p. e2727, 2019. DOI: 10.1002/etep.2727.